

Differentiable Model Compression via Pseudo Quantization Noise

Alexandre Défossez^{†1} Yossi Adi^{†1} Gabriel Synnaeve¹

Abstract

We propose to add independent pseudo quantization noise to model parameters during training to approximate the effect of a quantization operator. This method, DIFFQ, is differentiable both with respect to the unquantized parameters, and the number of bits used. Given a single hyper-parameter expressing the desired balance between the quantized model size and accuracy, DIFFQ can optimize the number of bits used per individual weight or groups of weights, in a single training. We experimentally verify that our method outperforms state-of-the-art quantization techniques on several benchmarks and architectures for image classification, language modeling, and audio source separation. For instance, on the Wikitext-103 language modeling benchmark, DIFFQ compresses a 16 layers transformer model by a factor of 8, equivalent to 4 bits precision, while losing only 0.5 points of perplexity. Code is available at: <https://github.com/facebookresearch/diffq>

1. Introduction

An important factor in the adoption of a deep learning model for real-world applications is how easily it can be pushed to remote devices. It has been observed that larger models usually lead to better performance, for instance with larger ResNets (He et al., 2016) achieving higher accuracies than smaller ones. In response, the community has worked toward smaller, and more efficient models (Tan & Le, 2019). Yet an EfficientNet-B3 is still almost 50MB, a considerable amount if the model is to be included in online applications, or should be updated with limited network capabilities. For other applications, such as language modeling (Vaswani et al., 2017) or source separation (Défossez et al., 2019), the typical model size is closer to 1GB, which rules out any kind of mobile usage.

The simplest method to reduce model size consists is de-

[†]Equal contribution ¹Facebook AI Research. Correspondence to: Alexandre Défossez <defossez@fb.com>.

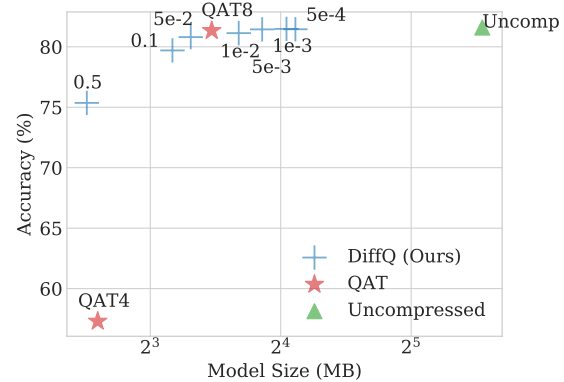


Figure 1. ImageNet results using EfficientNet-B3 model. We plot the model size vs. model accuracy using different penalty levels. We additionally, present the uncompressed models (uncomp.) and Quantization Aware Training (QAT) using 4 and 8 bits.

creasing the number of bits used to encode individual weights. For instance, using 16 bits floating point numbers halves the model size, while retaining a sufficient approximation of the set of real numbers, \mathbb{R} , to train with first-order optimization methods (Micikevicius et al., 2018). When considering lower precision, for instance, 8 or 4 bits, the set of possible values is no longer a good approximation of \mathbb{R} , hence preventing the use of first-order optimization methods. Specifically, uniform quantization requires using the `round` function, which has zero gradients wherever it is differentiable.

Quantization can be done as a post-processing step to regular training. However, errors accumulate in a multiplicative fashion across layers, leading to a possibly uncontrolled decrease in the model accuracy. Krishnamoorthi (2018) propose to use a gradient Straight-Through-Estimator (STE) (Bengio et al., 2013) in order to provide a non-zero gradient to the original weights. This allows the model to adapt to quantization during training and reduces the final degradation of performance. However, Fan et al. (2020) noticed instability and bias in the learned weights, as STE is not the true gradient to the function.

The nature of quantization noise has been extensively studied as part of Analog-to-Digital Converters (ADC). In particular, a useful assumption to facilitate the design of post-

processing filters for ADC is the independence of the input value and the “Pseudo Quantization Noise” (PQN), as formalized by [Widrow et al. \(1996\)](#). In this work, we show that it also applies to deep learning model quantization, and provides a simple framework in which the output and the quantized model size are both differentiable, without any use of STE. This allows to optimally set the number of bits used per individual weight (or group of weights) to a trade-off between size and accuracy, in a single training and at almost no extra cost. Even when the number of bits to use is fixed, we show that unlike STE, using independent pseudo quantization noise does not introduce bias in the gradient and achieves higher performance.

Our Contribution: (i) With DIFFQ, we propose to use pseudo quantization noise to approximate quantization at train time, as a differentiable alternative to STE, both with respect to the unquantized weights and number of bits used. (ii) We provide a differentiable model size estimate, so that given a single penalty level λ , DIFFQ optimizes the number of bits per weight or group of weights to achieve a given trade-off between model size and accuracy. (iii) We provide extensive experimental validation using various models (ConvNets and Transformers) and domains (image classification, language modeling, audio source separation). We demonstrate the efficiency of DIFFQ both in providing small footprint models with comparable performance to the uncompressed ones, together with easy and stable optimization, using only one sensitive hyper-parameter.

The paper is organized as follows: in Section 2 we present the relevant literature on the topic of quantization, while in Section 3 we provide a background on traditional quantization principles and discuss the limitations of STE based methods. In Section 4, we introduce our PQN based DIFFQ framework and training procedure. In Section 5, we empirically verify that the DIFFQ matches or surpasses the state-of-the-art on standard benchmarks in vision, natural language processing, and audio processing, along with a finer analysis of its behavior. Finally, we discuss open questions and future work in Section 6.

2. Related Work

Early network quantization methods focused on low-bitwidth networks such as BinaryNet ([Courbariaux et al., 2015; 2016](#)), XOR-Nets ([Rastegari et al., 2016](#)), or Ternary networks ([Li et al., 2016; Wu et al., 2018](#)). Although these methods produce highly quantized models, their performance is not on par with uncompressed ones. To improve accuracies, higher bitwidth quantization methods were studied ([Jung et al., 2019; Zhang et al., 2018a; Mishra et al., 2017](#)). These methods followed the STE approach ([Bengio et al., 2013](#)). STE allows the gradients to be backpropagated

through the quantizers and, thus, the network weights can be adapted with gradient descent ([Courbariaux et al., 2016](#)).

Variational approaches can be used to make the categorical distribution over quantized weights differentiable. [Louizos et al. \(2019\)](#) uses a Gumbel-softmax ([Jang et al., 2017](#)) but requires 2 hyper-parameters and has no bitwidth tuning. DIFFQ requires a single hyper-parameter while also supporting automatic bitwidth tuning. [Shayer et al. \(2018\)](#) relies on a Central Limit Theorem application, however this prevents weights from converging to a deterministic value, which would break the assumptions of the CLT. With DIFFQ, weights are free to converge to any optimal value. Finally [Ullrich et al. \(2017\)](#) uses a gaussian mixture model trained on top of the weights, adding significant complexity both in terms of code, and computation. In contrast, DIFFQ adds only a differentiable term to the loss, optimized along the rest of the model in a end-to-end fashion.

An alternative is to use a smoothed version of the quantization operator either with a trained meta-network ([Chen et al., 2019](#)), however as the smoothed operator converges to the true one, gradients will eventually be zero almost everywhere. [Gong et al. \(2019\)](#) use a meta-network to provide gradients despite quantization. However, their implementation for training the meta-network still relies on STE.

Additive noise injection has been studied by [Baskin et al. \(2018a\)](#), although only during the first few epochs, after which STE based approximation is used. This work was extended to non uniform quantization ([Baskin et al., 2018b](#)). In contrast, DIFFQ uses only noise injection, and as demonstrated in Section 5.4, achieves a better accuracy for an equivalent compression level than both methods. Non uniform quantization was also studied by [Polino et al. \(2018\)](#), but without differentiability with respect to the weights, with worse performance than DIFFQ (see Section 5.4).

An important contribution from DIFFQ is the automatic tuning of the bitwidth. [Wang et al. \(2019\); Elthakeb et al. \(2019\)](#) suggested learning a bitwidth assignment policy using reinforcement learning methods. In contrast, our method select bitwidth along training, using only first order optimization. [Jain et al. \(2019\); Esser et al. \(2020\)](#) proposed learning the quantizer step-size or dynamic-range using STE, but do not allow to select the bitwidth. [Uhlich et al. \(2020\)](#) proposed a re-parametrization that allows to select the bitwidth for each layer through first order optimization, while also relying on STE. The re-parametrization is more complex than the additive noise used in DIFFQ, and will suffer from the biased gradient of STE. Results presented in Section 5.4 show that DIFFQ achieves similar or better trade-offs between model size and accuracy. Besides, in the present work we also explore setting a bitwidth for individual groups of weights within each layer, rather than layer-wise.

The limitations of STE based methods for quantization were first noticed by Liu & Mattina (2019). They recommend using during training a linear combination of the unquantized and quantized weight, with the gradient flowing only through the unquantized contribution. In a similar spirit, Fan et al. (2020) sample for each layer and iteration whether to use the quantized or unquantized weight. Both methods reduce the bias from STE, but also remove some of the quantization noise during training. In contrast method allows to keep a full pseudo quantization noise without the STE bias.

A last line of related work is *Product Quantization* (Stock et al., 2019), where codewords are being learned to quantize blocks of weights rather than single weights. This method achieves a higher compression level than per-weight quantization but also requires carefully choosing the size of the codebooks for each layer. In contrast, our method requires only choosing a single hyper-parameter to balance between model size and accuracy. Besides, as noted by Fan et al. (2020), per-weight quantization and PQ can be combined.

3. Background

Let us consider a weight vector $w \in \mathbb{R}^d$, where $d \in \mathbb{N}$, typically the weights of convolution or linear layer. Each entry of the vector is typically coded over 32 bits with floating-point precision. We aim to reduce the number of possible states to 2^B , where $B \ll 32$ is the number of bits of precision. First, we assume $w_i \in [0, 1]$ for all $1 \leq i \leq d$. In practice, one would first normalize w as

$$\hat{w} = \frac{w - \min(w)}{\max(w) - \min(w)},$$

and provide the tuple $(\min(w), \max(w))$ separately as a 32 bits IEEE float. Given that for typical deep learning models $d \gg 1$, storing this range has a negligible cost. For readability, we describe the method for scalar values, however, this can be easily extended to vectors $w \in \mathbb{R}^d$.

3.1. Uniform quantization

The simplest quantization methods consist of taking 2^B points evenly spaced in the range $[0, 1]$ and round each entry of w to the nearest point. One then needs to store for each entry w_i , the index $\mathbf{Q}(w_i, B) \in [0, 2^B - 1]$ of its nearest point, which can be efficiently coded over B bits.

Formally, the index of the nearest quantized point is defined by the index function \mathbf{I} as

$$\mathbf{I}(x, B) = \text{round}(x \cdot (2^B - 1)), \forall x \in [0, 1]. \quad (1)$$

The quantized value is then decoded with the value function \mathbf{V} defined as

$$\mathbf{V}(q, B) = \frac{q}{2^B - 1}, \forall q \in [2^B - 1]. \quad (2)$$

Overall, the quantization process is defined as

$$\mathbf{Q}(x, B) = \mathbf{V}(\mathbf{I}(x, B), B), \forall x \in [0, 1], B \in \mathbb{N}_*. \quad (3)$$

While the intuitive definition of quantization is for an integer number of bits, we can extend the previous definitions to a real-valued number of bits $B \in \mathbb{R}_{*+}$. Note that variants of this scheme exist, for instance, symmetric uniform quantization, which enforces that 0 is always exactly represented (Krishnamoorthi, 2018).

3.2. Optimization of the quantized weights

The weight vector w is typically obtained through the process of training a predictor function parameterized by w , denote as f_w , to minimize a loss function L ,

$$\min_{w \in \mathbb{R}^d} L(f_w), \quad (4)$$

where $L(f_w)$ is the empirical risk over a given dataset. The process of quantizing a vector w over B bits introduces a quantization noise $\mathbf{N}(w, B) = \mathbf{Q}(w, B) - w$, which is unaware of the training objective L . Even if w is close to the optimum, $\mathbf{Q}(w, B)$ might deteriorate arbitrarily the performance of the predictor.

Thus, given a fixed budget of bits B , one would ideally like to minimize the empirical risk when considering the quantization process,

$$\min_{w \in \mathbb{R}^d} L(f_{\mathbf{Q}(w, B)}), \quad (5)$$

where $f_{\mathbf{Q}(w, B)}$ is the predictor function using the quantized model parameters.

Unfortunately, the gradients of $\mathbf{Q}(w, B)$ are zero over its definition domain because of the rounding operation, and as a result, it cannot be optimized using first-order optimization methods such as SGD or Adam (Kingma & Ba, 2015). One possible solution is to replace the Jacobian of $\mathbf{Q}(\cdot, B)$ with the identity matrix during the backward phase, as suggested in the STE method (Bengio et al., 2013). The STE method was applied to quantization as the Quantization Aware Training (QAT) technique by Krishnamoorthi (2018).

3.3. The instability and bias in STE

As described by Fan et al. (2020), following the STE approach can cause instability during training and bias in the models' gradients and weights. As a result optimization will fail to converge to the optimal value even on simple cases. To demonstrate that, consider the following 1D least-mean-square problem, where $B \in \mathbb{N}_*$, the optimal weight $w_* \in [0, 1]$ such that $\mathbf{Q}(w_*, B) \neq w_*$, and $\mathbf{Q}(w_*, B) \in (0, 1)$. Given a random variable $X \in \mathbb{R}$ with $\sigma^2 = \mathbb{E}[X^2]$ such that $0 < \sigma^2 < \infty$, we would like to

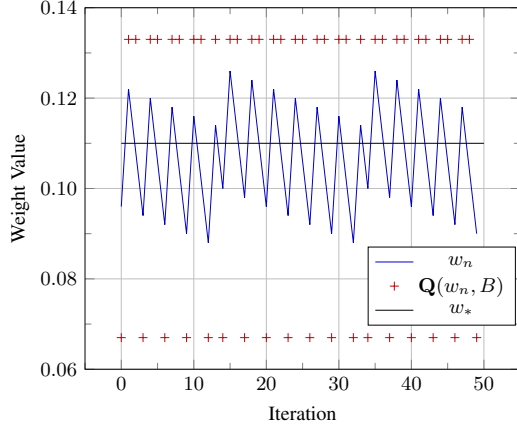


Figure 2. Using STE and SGD to optimize the 1D least-mean-square problem given by (6) (with $B = 4$ and $X = 1$ a.s.). $\mathbf{Q}(w_n, B)$ oscillates between the quantized value just above (w_+) and just under (w_-) the unquantized ground truth w_* , while w_n oscillates around the boundary $(w_+ + w_-)/2$. Diminishing the step size will reduce the oscillations of w_n , but will not reduce the scale of oscillations of the quantized value $\mathbf{Q}(w_n, B)$.

minimize the following using STE based QAT:

$$\min_{w \in [0,1]} L(w) := \mathbb{E} \left[\frac{1}{2} (X \mathbf{Q}(w, B) - X w_*)^2 \right]. \quad (6)$$

We immediately have that the optimum is achieved for $\mathbf{Q}(w, B) = \mathbf{Q}(w_*, B)$. Let us try to optimize (6) using SGD with STE starting from $w_0 = w_*$, with w_n the sequence of iterates. We call w_- and w_+ the quantized values just under and above w_* , and we assume without loss of generality that $\mathbf{Q}(w_*, B) = w_+$. The expected gradient with STE at iteration n is given by

$$G_n = \sigma^2(\mathbf{Q}(w_n, B) - w_*). \quad (7)$$

In particular, $G_0 = \sigma^2(w_+ - w_*) > 0$, and G_n will stay positive until $\mathbf{Q}(w_n, B) = w_-$. At this point, we will have $G_n < 0$, and will stay so until $\mathbf{Q}(w_n, B) = w_+$. Thus, we observe that using STE, $\mathbf{Q}(w_n, B)$ will oscillate between w_- and w_+ , while the optimal value is w_+ . The pattern of oscillation will depend on the learning rate and relative position of w_* within the segment $[w_-, w_+]$. Taking a smaller step size will reduce the amplitude of the oscillations of w_n , but not of $\mathbf{Q}(w_n, B)$, which is what interests us. Indeed, w_n oscillations are centered at the boundary $(w_+ + w_-)/2$. We provide one example of those oscillations on Figure 2 with $w_* = 0.11$, $B = 4$, $X = 1$ a.s. and a step size of 0.5.

Extrapolating to a model with millions of parameters, at any point in time, a significant fraction of the weights could be quantized to a suboptimal value due to the oscillations implied by the STE method. In the following section, we introduce DIFFQ, a method based on independent additive pseudo quantization noise, that does not suffer from such a

bias, while approximating well enough quantization noise to perform efficient quantization aware training.

4. Method

Pseudo quantization noise. A classical assumption in digital signal processing when working with quantized signals is that the quantization noise is approximated by independent uniform variables over $[-\Delta/2, \Delta/2]$ with $\Delta = \frac{1}{2^{B-1}}$ the quantization step. This approximation was studied in depth by (Widrow et al., 1996) as Pseudo Quantization Noise (PQN). Following this assumption, we define the *pseudo quantization function* $\tilde{\mathbf{Q}}$ for all $x \in \mathbb{R}$ and $B \in \mathbb{R}_{+*}$ as

$$\tilde{\mathbf{Q}}(x, B) = x + \frac{\Delta}{2} \cdot \mathcal{U}[-1, 1], \quad (8)$$

with $\mathcal{U}[-1, 1]$ an independent sample from the uniform distribution over $[-1, 1]$. This pseudo quantization function is differentiable with respect to x and B . Unlike QAT, this differentiability does not require an STE. It also provides a meaningful gradient with respect to the number of bits used B (extended to be real-valued).

If we look back at the example from Section 3.3, using now (8) instead of STE, the expected gradients for SGD become

$$\begin{aligned} G_n &= \mathbb{E} \left[x \cdot \left(\left(w_n + \frac{\Delta}{2} \cdot \mathcal{U}[-1, 1] \right) x - w_* x \right) \right] \\ &= \sigma^2(w_n - w_*). \end{aligned}$$

which cancels out for $w_n = w_*$, so that at convergence we indeed have $\mathbf{Q}(w_n, B) = \mathbf{Q}(w_*, B)$, i.e. the gradient estimate is unbiased and converges to the right solution.

Mixed precision. We used a single-precision B for all the entries of the weight vector w . One can instead use different values for different entries. Formally, the entries in w are grouped by considering $w \in \mathbb{R}^{g \times d/g}$ with g the group size and d/g the number of groups. We can then extend the definition of $\mathbf{Q}(w, B)$ given by (3) and (8) to use a number of bits b_s for the group s , with $b \in \mathbb{R}_{+*}^{d/g}$.

Training objective. Given $w \in \mathbb{R}^{g \times d/g}$ with g groups of d/g entries, and a number of bits $b \in \mathbb{N}_*^g$, we define the model size, expressed in MegaBytes (1MB = $8 \cdot 2^{20}$ bits)

$$\mathbf{M}(b) = \frac{g}{2^{23}} \sum_{s=1}^{d/g} b_s. \quad (9)$$

A typical objective of quantization is to achieve the best possible performance within a given model size budget or to achieve the smallest model size that reaches a given performance, i.e. we want to minimize with $b \in \mathbb{N}_*^{d/g}$, and $w \in \mathbb{R}^{g \times d/g}$ either,

$$\begin{aligned} \min_{w,b} L(f_{\mathbf{Q}(w,b)}), & \quad \text{or} \quad \min_{w,b} \mathbf{M}(b), \\ \text{s.t. } \mathbf{M}(b) \leq m. & \quad \text{s.t. } L(f_{\mathbf{Q}(w,b)}) \leq l. \end{aligned} \quad (10)$$

Table 1. Music source separation results for the Demucs model (Défossez et al., 2019). Results are presented for DIFFQ and QAT using 4 and 5 bits. We report Signal-to-Distortion Ratio (SDR) together with Model Size (M.S.).

	SDR \uparrow	M. S. (MB) \downarrow
UNCOMPRESSED	6.31	1014
QAT 4BITS	5.99	130
QAT 5BITS	6.27	162
DIFFQ ($\lambda=3e-4$)	6.28	120

We can relax b to be real valued, and replace \mathbf{Q} by our differentiable pseudo quantization function $\tilde{\mathbf{Q}}$. Then, following the *exact penalty method* (Bertsekas (1997), Section 4.2, Bertsekas (2014), Chapter 4), there is $\lambda(m) > 0$ (or $\lambda(l)$ for the right hand side problem), such that the left hand size problem is equivalent to

$$\min_{w,b} L(f_{\tilde{\mathbf{Q}}(w,b)}) + \lambda(m)\mathbf{M}(b), \quad (11)$$

which is fully differentiable with respect to w and b and can be optimized with first order optimization methods.

Parametrization. In practice, the number of bits used for each group $b \in \mathbb{R}_{*+}^g$ is obtained from a logit parameter $l \in \mathbb{R}^g$, so that we have

$$b = b_{\min} + \sigma(l)(b_{\max} - b_{\min}), \quad (12)$$

with σ is the sigmoid function, and b_{\min} and b_{\max} the minimal and maximal number of bits to use. The trainable parameter l is initialized so that we have $b = b_{\text{init}}$.

Evaluation and noise distribution. At evaluation time, we round the value b obtained from (11) as $\tilde{b} = \text{round}(b)$ and quantize w as $\mathbf{Q}(w, \tilde{b})$. Thus, the amount of quantization noise at evaluation time can be larger than the amount of noise injected at train time. We observed that using a noise distribution with larger support, such as Gaussian noise, makes the model more robust to this operation.

True model size. The mode size given by (9) is used at train time but does not account for part of the true model size. At evaluation time, we represent each layer weights by the indexes given by $\mathbf{I}(w, \tilde{b})$. For each layer in the network, we also store two 32 bits float numbers (coding the minimum and maximum scale). Finally, the actual value of \tilde{b} must be coded, as it is no longer a fixed constant. For each layer, we compute the maximum value of $C_s = \log_2(1 + \tilde{b}_s - b_{\min})$ over all groups $s \in \{1, \dots, d/g\}$. We encode once the value $\max(C)$ as an 8-bit integer, and for each group, we then encode $b_s - b_{\min}$ over $\max(C)$ bits. The true size for one layer, expressed in MegaBytes, is thus given by

$$\tilde{\mathbf{M}}(b) = \frac{1}{2^{23}} \left(2 \cdot 32 + 8 + \frac{d}{g} \max(C) + g \sum_{s=1}^{d/g} b_s \right) \quad (13)$$

5. Results

We present experimental results for audio source separation, image classification, and language modeling. We show that DIFFQ can systematically provide a model with comparable performance to the uncompressed one while producing a model with a smaller footprint than the baseline methods (STE based). We provide a finer analysis of different aspects of DIFFQ hyper-parameters and their impact on quantized models in Section 5.5. Both experimental code, and a generic framework usable with any architecture in just a few lines, are available on our Github¹. All hyper-parameters for optimization and model definition for all tasks are detailed in the Supplementary Material, Section A.

DIFFQ hyper-parameters For all experiments, we use $b_{\min} = 2$, $b_{\max} = 15$, $b_{\text{init}} = 8$ and Gaussian noise. We observed on most models that taking $b_{\min} < 2$ is unstable, with the notable exception of Resnet-20. We use a separate Adam optimizer (Kingma & Ba, 2015) for the logit parameters controlling the number of bits used, with a default momentum $\beta_1 = 0.9$ and decay $\beta_2 = 0.999$. We use the default learning rate $\alpha = 1e-3$ for all task, except language modeling where we use $\alpha = 1e-2$. The remaining hyper-parameters are λ , the amount of penalty applied to the model size, and g , the group size. When g is not mentioned, it is set to the default value $g = 8$, which we found to be the best trade-off between the model freedom and the overhead from storing the number of bits used for each group.

5.1. Music Source Separation

We use the Demucs architecture by Défossez et al. (2019) with 64 initial hidden channels. The baseline is enhanced to account for recent improvement from speech source separation (Défossez et al., 2020) and pitch/tempo shift augmentation (Cohen-Hadria et al., 2019). The model is trained on the standard MusDB benchmark (Raffi et al., 2017) for 180 epochs, and evaluated with the Signal-To-Distortion Ratio (SDR) metric (Vincent et al., 2006). The unquantized model is 1GB. We compare DIFFQ with QAT training with either 5 or 4 bits, with the results presented in Table 1. With 5 bits, QAT is able to replicate almost the same performance as the uncompressed model. However, trying to further compress the model to 4 bits precision leads to a sharp decrease of the SDR, losing 0.3 points, for a 130MB model. In contrast, DIFFQ achieves a model size of 120MB, with only a drop of 0.03 point of SDR compared to the uncompressed baseline.

5.2. Language Modeling

We trained a 16 layers transformer (Vaswani et al., 2017) based language model on the Wikitext-103 text corpus (Merity et al., 2016), following Baeovski & Auli (2019), and using the Fairseq framework (Ott et al., 2019). Results are pre-

¹<https://github.com/facebookresearch/diffq>

Table 2. Language modeling results for a 16 layer Transformer trained on Wikitext-103. We also test combining weight and activation quantization. We compared DIFFQ to QAT and Quant-Noise (QN) method proposed by Fan et al. (2020) (models with † were trained with a layer-drop of 0.2 (Fan et al., 2019)). Activations are quantized over 8 bits, with a per-channel scaling.

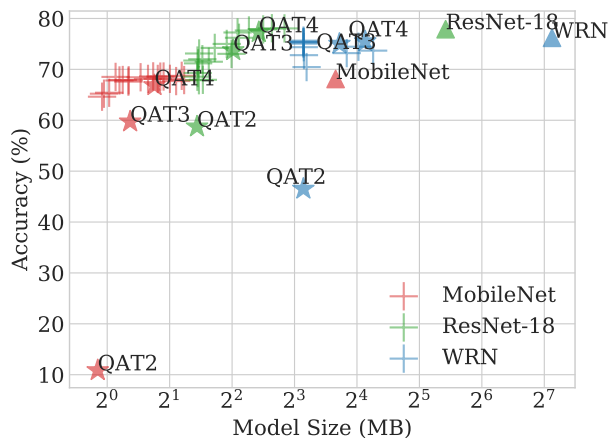
WEIGHTS	ACTIVATION	PPL ↓	M. S. (MB) ↓
UNCOMPRESSED	-	18.1	942
8 BITS	8 BITS	18.3	236
QAT 8BITS	8 BITS	19.7	236
QAT 4BITS	8 BITS	29.9	118
DIFFQ ($\lambda=1, g=16$)	8 BITS	18.0	182
DIFFQ ($\lambda=10, g=16$)	8 BITS	18.6	113
UNCOMPRESSED †	-	18.3	942
QN 8 BITS †	QN 8 BITS	18.7	236
QN 4 BITS †	QN 8 BITS	19.5	118

sented in Table 2. We compare to the Quant-Noise method by Fan et al. (2020), but use a reduced layer-drop (Fan et al., 2019) of 0.1 instead of 0.2. This both improves the baseline, as well as the performance of DIFFQ models. In order to further improve the performance of DIFFQ with layer-drop, we explicitly set the gradient for the number of bits parameters to zero for all layers that have been dropped. In order to test the compatibility of DIFFQ with efficient int8 kernels, we further quantize the activations to 8 bits using PyTorch native support (Paszke et al., 2019).

While QAT breaks down when trying to get to 4 bits precision (perplexity of 29.9), using DIFFQ allows to achieve an even lower model size (113MB vs. 118 MB for QAT 4 bits) with a perplexity closer to the uncompressed one (18.6, vs. 18.1 uncompressed). Even more interesting, with a lower penalty of 1, DIFFQ produces a model smaller than QAT 8 bits, and with a perplexity better than the baseline. While Quant-Noise significantly improves over QAT, it produces models that are both larger, and with worse perplexity than DIFFQ. Note that we did not use noise injection to emulate activation quantization, and it seems weight level noise injection was sufficient to make the model robust.

5.3. Image Classification

Next, we evaluated three image classification benchmarks: ImageNet (Deng et al., 2009), CIFAR-10 and CIFAR-100 (Krizhevsky et al., 2009). For CIFAR-10 and CIFAR-100 results are reported for MobileNet-v1 (Howard et al., 2017), ResNet-18 (He et al., 2016), and Wide-ResNet with 28x10, depth and width levels respectively (Zagoruyko & Komodakis, 2016). ImageNet results are reported using EfficientNet-B3 (Tan & Le, 2019) and DeiT-B (Touvron et al., 2020) models. See the Supplementary Material, Section A, for the hyper-parameters and augmentations used.



(a) CIFAR-100

Figure 3. Model accuracy and size on CIFAR-100 using MobileNet, ResNet-18, and WideResNet (WRN) models for various penalty levels using DIFFQ, QAT 4 and 8 models, and the baseline.

Table 3. Image classification results for the ImageNet benchmark. Results are presented for DIFFQ and QAT using 4 and 8 bits using the DeiT model (Touvron et al., 2020). We report Top-1 Accuracy (Acc.) together with Model Size (M.S.).

	TOP-1 Acc. (%) ↑	M.S. (MB) ↓
UNCOMPRESSED	81.8	371.4
QAT 4BITS	79.2	41.7
QAT 8BITS	81.6	82.9
DIFFQ ($\lambda=1e-2$)	82.0	45.7
DIFFQ ($\lambda=0.1$)	81.5	33.02

CIFAR10 & CIFAR-100. Results for CIFAR-100 are depicted in Figure 3. We compare DIFFQ to QAT using 2, 3, and 4 bits quantization. Performance of the uncompressed model is additionally presented as an upper-bound. To understand the effect of the penalty level λ on both model size and accuracy, we train models with DIFFQ using different penalty levels. Notice, as we decrease λ , model size increases together with model accuracy until it reaches a plateau in performance. Exact results are presented in Table B.1, in the Supplementary Material, along with the results on CIFAR-10, and a detailed analysis is in Section B.1.

Results suggest DIFFQ models reach comparable performance to the QAT models while producing models with a smaller footprint. When considering QAT with 2 bits quantization, DIFFQ archives large accuracy improvements while producing a model with equivalent size.

ImageNet. Results for ImageNet using DeiT-B model are presented in Table 3. We compared DIFFQ to QAT when training with 4 and 8 bits. Both QAT with 8 bits and DIFFQ

Table 4. Comparison of DIFFQ against baselines presented in Section 2. Each table section is for a specific dataset and model. We report accuracy (Acc.) and Model Size (M.S.). Sizes marked with \dagger are reported after Huffman coding, following Polino et al. (2018).

METHOD	Acc. \uparrow	M.S. \downarrow
CIFAR10 - ResNet-18		
DIFFQ (ours)	93.9	2.7 MB
NICE (Baskin et al., 2018a)	92.7	2.7 MB
UNIQ (Baskin et al., 2018b)	89.1	2.7 MB
CIFAR100 - Wide-ResNet		
DIFFQ (ours)	75.6	4.7 MB\dagger
Diff. Quant. (Polino et al., 2018)	49.3	7.9 MB \dagger
ImageNet - ResNet-18		
DIFFQ (ours)	69.4	5.3 MB
DQ (Uhlich et al., 2020)	70.1	5.4 MB
Meta-Quant (Chen et al., 2019)	60.3	1.3 MB
CIFAR-10 - ResNet-20		
DIFFQ (ours)	91.7	69 KB
DQ (Uhlich et al., 2020)	91.4	70 KB

reach comparable performance to the uncompressed model, while DIFFQ yields a model almost half of the size as QAT, however still bigger than QAT with 4 bits. When we increase λ , we get a smaller model-size than QAT with 4 bits but with better accuracy levels.

We evaluate the performance of DIFFQ on the memory-efficient architecture EfficientNet-B3 model on Figure 1. Those results are also presented in Table B.4 in the Supplementary Material. Both QAT 8 bits and DIFFQ achieves similar performance for equivalent model sizes, with a small drop compared to the uncompressed baseline. However, when considering QAT 4 bits, DIFFQ produces a smaller model with a significantly better accuracy level. In fact, for QAT 4, we noticed considerable instability close to the end of the training, see Section B.2 in the Supplementary Material for a more detailed analysis.

5.4. Comparison to related work

On Table 4, we compare to some of the related work presented in Section 2. Compared with the NICE (Baskin et al., 2018a) and UNIQ (Baskin et al., 2018b) methods, which also rely on additive noise, DIFFQ achieves significantly better accuracy for the same model size. We then compare to the differentiable quantization method by (Polino et al., 2018), which only optimizes the non uniform quantization points, not the pre-quantization weights. Following their practice, we report numbers after Huffman coding. We achieve a model almost half as small, with a gap of 25% in accuracy, which highlight that optimizing pre-quantization

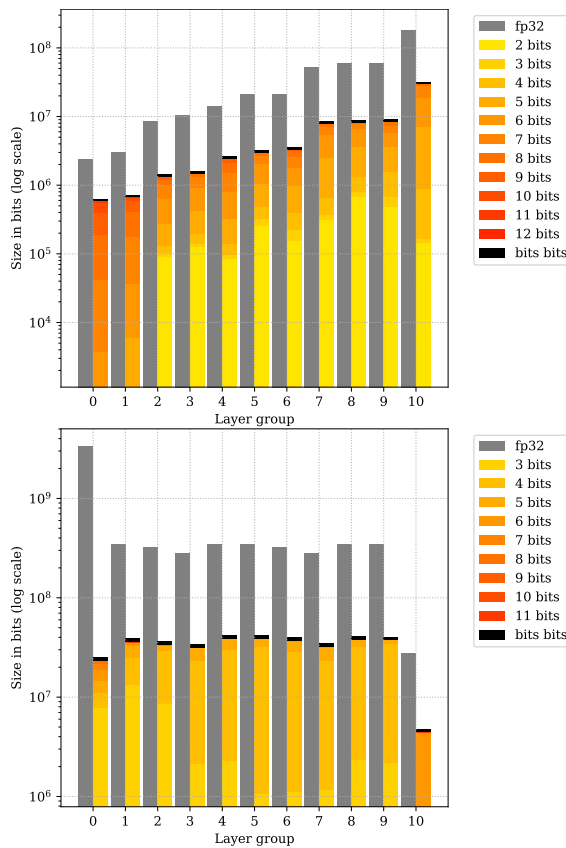


Figure 4. Layer groups wise size of the baseline EfficientNet-B3 (above) and DeiT (below) models (floating point 32 bits) and the quantized model with DIFFQ ($\lambda=5e-3$ for EfficientNet-B3, $\lambda=1e-2$ for DeiT) with cumulative bits per weights. Layers are grouped in increasing depth (0 is close to the input), “bits bits” shows the capacity needed to encode the weights’ bitwidth.

weights is more important than tuning a non uniform quantization grid. Meta-Quant (Chen et al., 2019) achieves smaller model size than DIFFQ, with 1 bit per weight, a regime where the PQN assumption breaks down, at the price of losing nearly 10% of accuracy. Finally, compared with the D.Q. method by Uhlich et al. (2020), we achieve comparable results on ImageNet with ResNet-18, and both smaller and more accurate models on CIFAR-10 with ResNet-20.

5.5. Analysis

In the following, we perform a finer analysis of the behavior of DIFFQ. First we look at the distribution of the number of bits used for different layers for various architectures. We then perform an ablation study, looking at the performance of DIFFQ without learning the number of bits, and the impact of the group size. Finally, we compare the difference in entropy of the learned models with QAT and DIFFQ.

Bits Histogram Figure 4 presents the weight bitwidth as-

Table 5. A comparison between QAT and DIFFQ while we consider a fixed number of bits for all model parameters, specifically using 2, 3, and 4 bits. We report Accuracy (Acc.) and Model Size (M.S.) for a ResNet-18 model trained on CIFAR-100.

	Acc. (%) \uparrow	M. S. (MB) \downarrow
UNCOMPRESSED	77.9	42.81
QAT 2BITS	58.7	2.72
QAT 3BITS	73.7	4.05
QAT 4BITS	77.3	5.39
DIFFQ 2BITS	66.6	2.72
DIFFQ 3BITS	76.7	4.05
DIFFQ 4BITS	77.5	5.39

segmentation over layer groups for the EfficientNet-B3 (Tan & Le, 2019) and DeiT (Touvron et al., 2020) models trained on ImageNet. The capacity distribution over depth for ConvNets (EfficientNet-B3) and Transformers (DeiT) are different (fp32 shows uncompressed capacity). Notice, that the quantization trends are different too: for the ConvNet, smaller bitwidths are used for deeper layers of the model while large bitwidth is more common in the first layers (except for the last linear layer which seems to need some precision). For the Transformer, this effect of varying quantization by layer is similar but less pronounced.

Ablation Recall, in Section 3.3 we demonstrated the instability of following STE for optimization. In Table 5 we compare QAT to DIFFQ for a ResNet-18 trained on CIFAR-100, where we consider a fixed number of bits for all model parameters. DIFFQ outperforms QAT, where this is especially noticeable while using 2 bits quantization, in which training is less stable for QAT. The same occurs for other architectures (MobileNet, Wide-ResNet) and datasets (CIFAR-10) as shown in Table B.3, in the Supplementary.

Next, we evaluated the affect of the group-size, g , on model size and accuracy, by optimizing DIFFQ models using $g \in \{1, 4, 8, \infty\}$. When $g = \infty$, we use a single group for the entire layer. Results for ResNet-18 using CIFAR-100 are summarized in Figure 5. Interestingly, we observed that increasing g , yields in a smaller model size on the expense of a minor decrease in performance. However, when setting $g = \infty$ model performance (model size and accuracy) is comparable to $g = 8$ for this task.

DIFFQ maximizes entropy usage The model size given by (13) is obtained with a traditional encoding of the quantized model. However, more efficient coding techniques exist when the entropy of the data is low, such as Huffman coding (Huffman, 1952). Using the ZLib library, we obtain an estimate of the Huffman compressed model size after quantization. For instance, for the language model described in Table 2, the QAT 8 model gets further compressed from 236MB to 150MB, showing that the entropy of its quantized

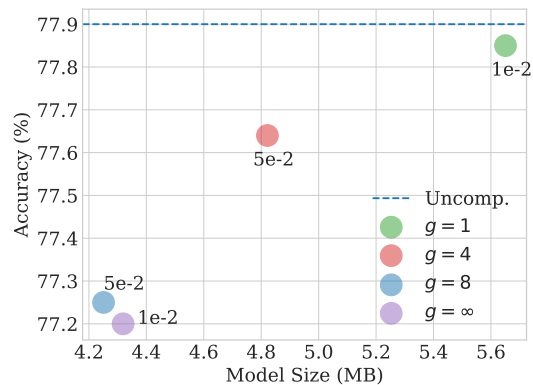


Figure 5. DIFFQ results with various groups sizes ($g \in \{1, 4, 8, \infty\}$). $g = \infty$ refers to a single group for the entire layer. For reference, we report the accuracy of the uncompressed model (42.8 MB). Models are Resnet-18 trained on CIFAR-100.

weight is significantly lower than the maximal one for 8 bits integers. However, the DIFFQ model naive size is 113MB, and after compression by ZLib, gets to 122MB. This is a sign that the underlying entropy is close to its maximal value, with ZLib adding only overhead for no actual gain.

In (11), we only penalize the naive number of bits used, while asking for the best possible accuracy. In that case, the model maximally use the entropy capabilities for a given number of bits. An interesting line of research would be to replace the model size (9) to account for the actual entropy of the data. We leave that for further research.

6. Discussion

We presented DIFFQ, a novel and simple differentiable method for model quantization via pseudo quantization noise addition to models’ parameters. Given a single hyperparameter that quantifies the desired trade-off between model size and accuracy, DIFFQ can optimize the number of bits used for each trainable parameter or group of parameters during model training.

We conduct expensive experimental evaluations on various domains using different model architectures. Results suggest that DIFFQ is superior to the baseline methods on several benchmarks from various domains. On ImageNet, Wikitext-103, and MusDB, we achieve a model size equivalent or smaller to a 4 bits quantized model, while retaining the same performance as the unquantized baseline.

For future work, we consider adapting the model size penalty to account for Huffman encoding, which could allow to further reduce the model size when it is gzipped. Another line of work would be using PQN to improve activation quantization. While 8-bits activations are well supported, this could open up the way to a 4-bits kernel.

References

- Baevski, A. and Auli, M. Adaptive input representations for neural language modeling. In *Proc. of the International Conference on Learning Representations*, 2019.
- Baskin, C., Liss, N., Chai, Y., Zheltonozhskii, E., Schwartz, E., Giryes, R., Mendelson, A., and Bronstein, A. M. Nice: Noise injection and clamping estimation for neural network quantization. *arXiv preprint arXiv:1810.00162*, 2018a.
- Baskin, C., Schwartz, E., Zheltonozhskii, E., Liss, N., Giryes, R., Bronstein, A. M., and Mendelson, A. Uniq: Uniform noise injection for non-uniform quantization of neural networks. *arXiv preprint arXiv:1804.10969*, 2018b.
- Bengio, Y., Léonard, N., and Courville, A. Estimating or propagating gradients through stochastic neurons for conditional computation. *arXiv preprint arXiv:1308.3432*, 2013.
- Bertsekas, D. P. Nonlinear programming. *Journal of the Operational Research Society*, 48(3):334–334, 1997.
- Bertsekas, D. P. *Constrained optimization and Lagrange multiplier methods*. Academic press, 2014.
- Chen, S., Wang, W., and Pan, S. J. Metaquant: Learning to quantize by learning to penetrate non-differentiable quantization. In *Advances in Neural Information Processing Systems*, 2019.
- Cohen-Hadria, A., Roebel, A., and Peeters, G. Improving singing voice separation using deep u-net and wave-u-net with data augmentation. In *27th European Signal Processing Conference (EUSIPCO)*. IEEE, 2019.
- Courbariaux, M., Bengio, Y., and David, J.-P. Binaryconnect: Training deep neural networks with binary weights during propagations. *arXiv preprint arXiv:1511.00363*, 2015.
- Courbariaux, M., Hubara, I., Soudry, D., El-Yaniv, R., and Bengio, Y. Binarized neural networks: Training deep neural networks with weights and activations constrained to +1 or -1. *arXiv preprint arXiv:1602.02830*, 2016.
- Défosssez, A., Usunier, N., Bottou, L., and Bach, F. Music source separation in the waveform domain. *arXiv preprint arXiv:1911.13254*, 2019.
- Défosssez, A., Synnaeve, G., and Adi, Y. Real time speech enhancement in the waveform domain. In *Proc. of Inter-speech*, 2020.
- Deng, J., Dong, W., Socher, R., Li, L.-J., Li, K., and Fei-Fei, L. ImageNet: A Large-Scale Hierarchical Image Database. In *CVPR*, 2009.
- Elthakeb, A., Pilligundla, P., Mireshghallah, F., Yazdanbakhsh, A., Gao, S., and Esmaeilzadeh, H. Releq: An automatic reinforcement learning approach for deep quantization of neural networks. In *NeurIPS ML for Systems workshop, 2018*, 2019.
- Esser, S. K., McKinstry, J. L., Bablani, D., Appuswamy, R., and Modha, D. S. Learned step size quantization. In *Proc. of the International Conference on Learning Representations*, 2020.
- Fan, A., Grave, E., and Joulin, A. Reducing transformer depth on demand with structured dropout. In *Proc. of the International Conference on Learning Representations*, 2019.
- Fan, A., Stock, P., Graham, B., Grave, E., Gribonval, R., Jegou, H., and Joulin, A. Training with quantization noise for extreme model compression. In *ICLR 2021*, 2020.
- Gong, R., Liu, X., Jiang, S., Li, T., Hu, P., Lin, J., Yu, F., and Yan, J. Differentiable soft quantization: Bridging full-precision and low-bit neural networks. In *Proceedings of the IEEE International Conference on Computer Vision*, 2019.
- He, K., Zhang, X., Ren, S., and Sun, J. Deep residual learning for image recognition. In *Proceedings of the IEEE conference on computer vision and pattern recognition*, 2016.
- Howard, A. G., Zhu, M., Chen, B., Kalenichenko, D., Wang, W., Weyand, T., Andreetto, M., and Adam, H. Mobilenets: Efficient convolutional neural networks for mobile vision applications. *arXiv preprint arXiv:1704.04861*, 2017.
- Huffman, D. A. A method for the construction of minimum-redundancy codes. *Proceedings of the IRE*, 40(9):1098–1101, 1952. doi: 10.1109/JRPROC.1952.273898.
- Jain, S. R., Gural, A., Wu, M., and Dick, C. H. Trained quantization thresholds for accurate and efficient fixed-point inference of deep neural networks. *arXiv preprint arXiv:1903.08066*, 2019.
- Jang, E., Gu, S., and Poole, B. Categorical reparameterization with gumbel-softmax. In *Proc. of the International Conference on Learning Representations*, 2017.
- Jung, S., Son, C., Lee, S., Son, J., Han, J.-J., Kwak, Y., Hwang, S. J., and Choi, C. Learning to quantize deep networks by optimizing quantization intervals with task loss. In *Proceedings of the IEEE/CVF Conference on Computer Vision and Pattern Recognition*, pp. 4350–4359, 2019.
- Kingma, D. P. and Ba, J. Adam: A method for stochastic optimization. In *Proc. of the International Conference on Learning Representations*, 2015.

- Krishnamoorthi, R. Quantizing deep convolutional networks for efficient inference: A whitepaper. *arXiv preprint arXiv:1806.08342*, 2018.
- Krizhevsky, A., Hinton, G., et al. Learning multiple layers of features from tiny images. Technical report, University of Toronto, 2009.
- Li, F., Zhang, B., and Liu, B. Ternary weight networks. *arXiv preprint arXiv:1605.04711*, 2016.
- Liu, Z.-G. and Mattina, M. Learning low-precision neural networks without straight-through estimator (ste). *arXiv preprint arXiv:1903.01061*, 2019.
- Loshchilov, I. and Hutter, F. Decoupled weight decay regularization. In *Proc. of the International Conference on Learning Representations*, 2019.
- Louizos, C., Reisser, M., Blankevoort, T., Gavves, E., and Welling, M. Relaxed quantization for discretized neural networks. In *Proc. of the International Conference on Learning Representations*, 2019.
- Merity, S., Xiong, C., Bradbury, J., and Socher, R. Pointer sentinel mixture models. In *Proc. of the International Conference on Learning Representations*, 2016.
- Micikevicius, P., Narang, S., Alben, J., Diamos, G., Elsen, E., Garcia, D., Ginsburg, B., Houston, M., Kuchaiev, O., Venkatesh, G., et al. Mixed precision training. In *Proc. of the International Conference on Learning Representations*, 2018.
- Mishra, A., Nurvitadhi, E., Cook, J. J., and Marr, D. Wrpn: Wide reduced-precision networks. In *Proc. of the International Conference on Learning Representations*, 2017.
- Ott, M., Edunov, S., Baevski, A., Fan, A., Gross, S., Ng, N., Grangier, D., and Auli, M. fairseq: A fast, extensible toolkit for sequence modeling. In *Proceedings of NAACL-HLT 2019: Demonstrations*, 2019.
- Paszke, A. et al. Pytorch: An imperative style, high-performance deep learning library. In *Advances in Neural Information Processing Systems 32*, 2019.
- Polino, A., Pascanu, R., and Alistarh, D. Model compression via distillation and quantization. In *Proc. of the International Conference on Learning Representations*, 2018.
- Rafii, Z., Liutkus, A., Stöter, F.-R., Mimilakis, S. I., and Bittner, R. The musdb18 corpus for music separation, 2017.
- Rastegari, M., Ordonez, V., Redmon, J., and Farhadi, A. Xnor-net: Imagenet classification using binary convolutional neural networks. In *European conference on computer vision*, pp. 525–542. Springer, 2016.
- Shayer, O., Levi, D., and Fetaya, E. Learning discrete weights using the local reparameterization trick. In *Proc. of the International Conference on Learning Representations*, 2018.
- Stock, P., Joulin, A., Gribonval, R., Graham, B., and Jégou, H. And the bit goes down: Revisiting the quantization of neural networks. In *Proc. of the International Conference on Learning Representations*, 2019.
- Szegedy, C., Vanhoucke, V., Ioffe, S., Shlens, J., and Wojna, Z. Rethinking the inception architecture for computer vision. In *Proceedings of the IEEE conference on computer vision and pattern recognition*, pp. 2818–2826, 2016.
- Tan, M. and Le, Q. V. Efficientnet: Rethinking model scaling for convolutional neural networks. In *Proc. of the International Conference on Machine Learning*, 2019.
- Tieleman, T. and Hinton, G. Lecture 6.5-rmsprop: Divide the gradient by a running average of its recent magnitude, 2012.
- Touvron, H., Cord, M., Douze, M., Massa, F., Sablayrolles, A., and Jégou, H. Training data-efficient image transformers & distillation through attention. *arXiv preprint arXiv:2012.12877*, 2020.
- Uhlich, S., Mauch, L., Cardinaux, F., Yoshiyama, K., Garcia, J. A., Tiedemann, S., Kemp, T., and Nakamura, A. Mixed precision dnns: All you need is a good parametrization. In *Proc. of the International Conference on Learning Representations*, 2020.
- Ullrich, K., Meeds, E., and Welling, M. Soft weight-sharing for neural network compression. In *Proc. of the International Conference on Learning Representations*, 2017.
- Vaswani, A., Shazeer, N., Parmar, N., Uszkoreit, J., Jones, L., Gomez, A. N., Kaiser, L., and Polosukhin, I. Attention is all you need. In *Proc. of Neural Information Processing Systems*, 2017.
- Vincent, E., Gribonval, R., and Févotte, C. Performance measurement in blind audio source separation. *IEEE Transactions on Audio, Speech and Language Processing*, 2006.
- Wang, K. et al. Haq: Hardware-aware automated quantization with mixed precision. In *Proceedings of the IEEE/CVF Conference on Computer Vision and Pattern Recognition*, pp. 8612–8620, 2019.
- Widrow, B., Kollar, I., and Liu, M.-C. Statistical theory of quantization. *IEEE Transactions on instrumentation and measurement*, 45(2):353–361, 1996.
- Wightman, R. Pytorch image models. <https://github.com/wlightman/pytorch-image-models>, 2019.

- Wu, S., Li, G., Chen, F., and Shi, L. Training and inference with integers in deep neural networks. In *Proc. of the International Conference on Learning Representations*, 2018.
- Yun, S., Han, D., Oh, S. J., Chun, S., Choe, J., and Yoo, Y. Cutmix: Regularization strategy to train strong classifiers with localizable features. In *Proceedings of the IEEE/CVF International Conference on Computer Vision*, pp. 6023–6032, 2019.
- Zagoruyko, S. and Komodakis, N. Wide residual networks. *arXiv preprint arXiv:1605.07146*, 2016.
- Zhang, D., Yang, J., Ye, D., and Hua, G. Lq-nets: Learned quantization for highly accurate and compact deep neural networks. In *Proceedings of the European conference on computer vision (ECCV)*, pp. 365–382, 2018a.
- Zhang, H., Cisse, M., Dauphin, Y. N., and Lopez-Paz, D. mixup: Beyond empirical risk minimization. In *Proc. of the International Conference on Learning Representations*, 2018b.

Supplementary Material for

Differentiable Model Compression via Pseudo Quantization Noise

We provide in Section A all the details on the exact hyper-parameters, models, and datasets used for the results in Section 5 of the main paper. Then, we provide supplementary results in Section B, in particular tables for the scatter plots given on Figures 1 and 3. Finally, we present the code provided along with this Supplementary Material, in the `code` folder.

A. Detailed experimental setup

All experiments are conducted using NVIDIA V100 GPUs with either 16GB or 32GB RAM, depending on the applications (with language modeling requiring larger GPUs.). For all models trained with QAT or DIFFQ, we do not quantize tensors with a size under 0.01 MB (0.1 MB for the DeiT model).

A.1. Music Source Separation

We train a Demucs source separation model (Défossez et al., 2019) with a depth of 6 and 64 initial hidden channels, on the MusDB dataset (Rafii et al., 2017)². Following Défossez et al. (2020), we upsample the input audio by a factor of 2 before feeding it to the model and downsample the output by a factor of 2 before computing the loss. Following Cohen-Hadria et al. (2019), we also use pitch-shift/tempo stretch data augmentation using the `soundstretch` package³. A batch goes through this transformation with a probability of 20%, the tempo is changed by a uniform fractional amount between -12% and +12%. The pitch is shifted by at most 2 semitones. . Those data augmentation strongly improved the baseline. We train for 180 epochs, with a batch size of 64 and Adam (Kingma & Ba, 2015) with a learning rate of $3e-4$. All other training details are exactly as in (Défossez et al., 2019).

A.2. Language Modeling

We trained a 16 layers transformer (Vaswani et al., 2017) based language model on the Wikitext-103 text corpus (Merity et al., 2016)⁴, following Baevski & Auli (2019), and using the `Fairseq` framework (Ott et al., 2019). We used the hyper-parameters and the script provided by (Fan et al., 2020) in the `Fairseq` repository⁵, however, and unlike what they mention in their paper, this script does not include layer drop (Fan et al., 2019). For DIFFQ, we tried the penalty levels λ in $\{1, 5, 10\}$, with group size 8, as well as $\lambda = 10$ and $g = 16$.

Tied weights and DIFFQ. The model we trained was configured so that the word embedding in the first layer and the weight of the adaptive softmax are bound to the same value. It is important to detect such bounded parameters with DIFFQ, as otherwise, a different number of bits could be used for what is in fact, the very same tensor. Not only do we use a single bits logit parameter when a parameter tensor is reused multiple times, but for each forward, we make sure that the pseudo quantization noise is sampled only once and reused appropriately. Failure to do so led to a significant worsening of the performance at validation time.

A.3. Image classification

CIFAR10/100. On the CIFAR10/100 datasets, we train 3 different models: MobileNet-v1 (Howard et al., 2017), ResNet-18 (He et al., 2016), and a Wide-ResNet with 28x10 depth and width levels respectively (Zagoruyko & Komodakis, 2016). All experiments are conducted on a single GPU with a batch size of 128, SGD with a learning rate of 0.1, momentum of 0.9, weight decay of $5e-4$. The learning rate is decayed by a factor of 0.2 every 60 iterations. To generate Figure 3, we evaluated DIFFQ for λ in $\{0.01, 0.05, 0.1, 0.5, 1, 5\}$ and the group size g in $\{4, 8, 16\}$.

The dataset has been obtained from the `torchvision` package⁶. The input images are augmented with a random crop of size 32 with padding of 4, and a random horizontal flip. The RGB pixel values are normalized to mean 0 and standard

²<https://sigsep.github.io/datasets/musdb.html>

³<https://www.surina.net/soundtouch/soundstretch.html>

⁴<https://blog.einstein.ai/the-wikitext-long-term-dependency-language-modeling-dataset/>

⁵https://github.com/pytorch/fairseq/tree/master/examples/quant_noise

⁶<https://github.com/pytorch/vision>

deviation 1. We use the default split between train and valid as obtained from the `torchvision` package.

ImageNet. We train an EfficientNet as implemented by (Wightman, 2019), as well as a DeiT vision transformer (Touvron et al., 2020) on the ImageNet dataset (Deng et al., 2009)⁷. We use the original dataset split between train and valid. The images go through a random resize crop to 300px, a random horizontal flip, and pixel RGB values are normalized to have zero mean and unit variance.

ImageNet - EfficientNet. We trained for 100 epochs, using RMSProp (Tieleman & Hinton, 2012) as implemented in the `timm` package⁸ with a learning rate of 0.0016, a weight decay of $1e-5$ and a momentum of 0.9. The learning rate is decayed by a factor of 0.9875 with every epoch. As a warmup, the learning rate is linearly scaled from 0 to 0.0016 over the first 3 epochs. Following (Wightman, 2019), we evaluate with an exponential moving average of the weights of the model, with a decay of 0.99985. We use the random erase augmentation from (Wightman, 2019), as well as cutmix (Yun et al., 2019), with a probability of 0.2 and parameter to the beta distribution of 0.2. All the models are trained on 8 GPUs. For DIFFQ, we used the penalties λ in $\{5e-4, 1e-3, 5e-3, 1e-2, 5e-2, 0.1, 0.5\}$ and the default group size $g = 8$.

ImageNet - DeiT. We use the official DeiT implementation by Touvron et al. (2020)⁹, with the default training parameters, but without exponential moving averaging of the weights. More precisely, we trained for 300 epochs over 16 GPUs, with a batch size per GPU of 64, AdamW (Loshchilov & Hutter, 2019), a weight decay of 0.05, learning rate of $5e-4$, cosine learning rate scheduler, a learning rate warmup from $1e-6$ over 5 epochs and label smoothing (Szegedy et al., 2016). As data augmentation, we used color-jitter, random erase, and either cutmix or mixup (Zhang et al., 2018b).

For DIFFQ, we tested the penalty λ in $\{1e-3, 1e-2, 0.1, 0.5, 1, 5\}$, and group size g in $\{1, 4, 8\}$. We use a minimum number of bits of 3, instead of 2, as this led to better stability. We use Adam (Kingma & Ba, 2015) to optimize the bits parameters, with a learning rate of $5e-4$.

B. Supplementary results

Table B.1. Detailed results of QAT and DIFFQ on the CIFAR-10/100 datasets. For each architecture and dataset, we provide the performance of the baseline, QAT models with 2 to 4 bits, and two DIFFQ runs: v1. is the smallest model that is within a small range of the baseline performance, v2. is the best model of comparable size with QAT 2 bits, selected from the pool of candidates described in Section A.3. For Wide-ResNet, we report a single variant of DIFFQ, as it is both the smallest and the one with the best accuracy.

		MOBILENET		RESNET-18		WIDERESNET	
		Acc. (%) \uparrow	M. S. (MB) \downarrow	Acc. (%) \uparrow	M. S. (MB) \downarrow	Acc. (%) \uparrow	M. S. (MB) \downarrow
CIFAR-10	UNCOMPRESSED	90.9	12.3	95.3	42.7	95.3	139.2
	QAT 2BITS	78.1	0.88	87.2	2.70	70.8	8.81
	QAT 3BITS	88.2	1.26	94.0	4.03	94.3	13.16
	QAT 4BITS	90.1	1.64	95.0	5.36	94.4	17.50
	DIFFQ v1	90.3	0.94	94.9	3.17	94.1	8.81
	DIFFQ v2	87.9	0.91	93.9	2.71	94.1	8.81
CIFAR-100	UNCOMPRESSED	68.1	12.6	77.9	42.8	76.2	139.4
	QAT 2BITS	10.9	0.91	58.7	2.72	46.5	8.83
	QAT 3BITS	59.7	1.29	73.7	4.05	75.0	13.18
	QAT 4BITS	66.9	1.69	77.3	5.39	75.5	17.53
	DIFFQ v1	68.5	1.10	77.6	4.82	75.3	8.83
	DIFFQ v2	64.6	0.94	71.7	2.72	75.6	8.84

B.1. CIFAR-10/100

We report on Table B.1 the results on the CIFAR10/100 datasets, which are shown for CIFAR100 in Figure 3 in the main paper. Results are presented using MobileNet-v1, ResNet-18, and WideResNet. For CIFAR100 the presented results used for creating Figure 3 in the main paper. As we cannot show all the DIFFQ runs, we selected for each model and dataset two versions: v1 is the smallest model that has an accuracy comparable to the baseline (accuracy is greater than $1 - 1/100$ times the baseline accuracy), while v2 is the model with the highest accuracy that is comparable in size with the QAT 2 bits model

⁷<http://www.image-net.org/>

⁸<https://github.com/rwightman/pytorch-image-models>

⁹<https://github.com/facebookresearch/deit>

(size must be smaller than $1 + 1/100$ times the baseline size, except for MobileNet, for which we had to allow a 4% relative increase in size. The penalty and group size selected with this procedure is displayed on Table B.2.

Table B.2. Penalty λ and group size g for the v1 and v2 DIFFQ models reported on Table B.1

		MOBILENET		RESNET-18		WIDERESNET	
		λ	g	λ	g	λ	g
CIFAR-10	DIFFQ v1	1	16	0.1	8	5	16
	DIFFQ v2	5	8	5	4	5	16
CIFAR-100	DIFFQ v1	1	16	0.05	4	5	16
	DIFFQ v2	5	16	5	8	1	16

Looking first at v1 models, we achieve on all tasks and datasets a model that is competitive with the baseline (sometimes even better), with a model size that is smaller than a QAT 4 bits model (for instance more than 2MB saved on a ResNet-18 trained on CIFAR-10 compared to QAT 4 bits, for the same accuracy).

Now for v2, first note that as the minimum number of bits used by DIFFQ is exactly 2, it is not possible here to make a model smaller than QAT 2 bits. However, even with as little as 0.01 MB extra, DIFFQ can get up to 30% increase in accuracy compared to QAT 2 bits (for a Wide ResNet). On all architecture and datasets, the gain from DIFFQ over QAT 2 bits is at least 10% accuracy. This confirms in practice the bias of STE-based methods when the number of bits is reduced, a bias that we already demonstrated in theory in Section 3.3. In particular, it is interesting that the largest improvement provided by DIFFQ is for the Wide ResNet model, which should be the easiest to quantize. But having the largest number of weights, it is also likely the one that is the most sensitive to the oscillations of QAT quantized weights described in Section 3.3.

Next, in Table B.3 we compare QAT against DIFFQ for model quantization using a fixed number of bits. These results are complementary to Table 5 in the main paper where we report results for CIFAR-100 using ResNet-18 model only.

Table B.3. A comparison between QAT and DIFFQ while we consider a fixed number of bits for all model parameters, specifically using 2, 3, and 4 bits. Results are reported for CIFAR-10 and CIFAR-100 using MobileNet-v1, ResNet-18. and WideResNet. We report Accuracy (Acc.) and Model Size (M.S.).

		MOBILENET		RESNET-18		WIDERESNET	
		Acc. (%) \uparrow	M. S. (MB) \downarrow	Acc. (%) \uparrow	M. S. (MB) \downarrow	Acc. (%) \uparrow	M. S. (MB) \downarrow
CIFAR-10	UNCOMPRESSED	90.9	12.3	95.3	42.8	95.3	139.4
	QAT 2BITS	78.1	0.88	87.2	2.70	70.8	8.81
	QAT 3BITS	88.2	1.26	94.0	4.03	94.3	13.16
	QAT 4BITS	90.1	1.64	95.0	5.36	94.4	17.50
	DIFFQ 2BITS	84.1	0.88	92.3	2.70	94.4	8.81
	DIFFQ 3BITS	89.7	1.26	94.4	4.03	94.4	13.16
	DIFFQ 4BITS	90.4	1.64	95.1	5.36	94.6	17.50
CIFAR-100	UNCOMPRESSED	68.1	12.6	77.9	42.8	76.2	139.4
	QAT 2BITS	10.9	0.91	58.7	2.72	46.5	8.82
	QAT 3BITS	59.7	1.29	73.7	4.05	75.0	13.18
	QAT 4BITS	66.9	1.69	77.3	5.39	75.5	17.53
	DIFFQ 2BITS	17.2	0.91	66.6	2.72	72.8	8.82
	DIFFQ 3BITS	60.1	1.29	76.7	4.05	76.9	13.18
	DIFFQ 4BITS	66.8	1.69	77.5	5.39	76.9	17.53

B.2. EfficientNet-b3 on ImageNet

On Table B.4 we report the results for training EfficientNet-b3 (Tan & Le, 2019) on the ImageNet dataset, matching the results reported on Figure 1.

As previously, we selected two versions of DIFFQ, one matching the size of QAT 8bits, and one smallest than QAT 4 bits. At 8 bits, DIFFQ achieves the same accuracy as the uncompressed baseline, for a slightly smaller model than QAT 8bits. As we lower the number of bits, we again see a clear advantage for DIFFQ, with both a smaller model (5.7MB against 6.1MB) than QAT 4bits, and significantly higher accuracy (76.8% vs. 57.3%).

The lower accuracy for QAT4 on ImageNet led us to take a closer look at the model performance. Figure 6 depicts the model accuracy as a function of the number of epochs for both QAT4 and DIFFQ. Notice, similarly to the toy example presented in

Table B.4. Image classification results for the ImageNet benchmark. Results are presented for DIFFQ and QAT using 4 and 8 bits using the EfficientNet-b3 model (Tan & Le, 2019). We report Top-1 Accuracy (Acc.) together with Model Size (M.S.).

	TOP-1 ACC. (%) \uparrow	M.S. (MB) \downarrow
UNCOMPRESSED	81.6	46.7
QAT 4BITS	57.3	6.3
QAT 8BITS	81.3	12.0
DIFFQ ($\lambda=0.5$)	75.4	5.7
DIFFQ ($\lambda=5e-2$)	80.8	9.92

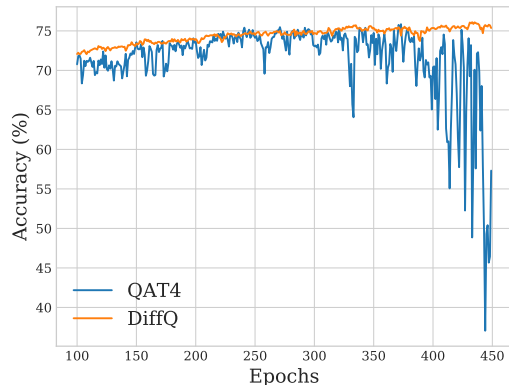


Figure 6. Model accuracy vs. epochs for ImageNet using EfficientNet-b3. Results are presented for both QAT4 and DIFFQ.

Section 3.3 training with QAT4 creates instability in the model optimization (especially near model convergence), which leads to significant differences in performance across adjacent epochs. When considering DIFFQ, model optimization is stable and no such differences are observed.

B.3. Activation Quantization for Language Modeling

In Table B.5 we report language modeling results for a 16-layers Transformer models while applying activation quantization. Unlike the results in Table 2 where we used per-channel activation quantization, here we report results with a histogram quantizer. Additionally when considering histogram quantizer, results suggest DIFFQ is superior to both QAT and QN when considering both model size and model performance.

Table B.5. Language modeling results for a 16 layer Transformer trained on Wikitext-103. We also test combining weight and activation quantization using a histogram quantizer. We compared DIFFQ to QAT and Quant-Noise (QN) method proposed by Fan et al. (2020) (models with \dagger were trained with layer drop (Fan et al., 2019)).

WEIGHTS	ACTIVATION	PPL \downarrow	M. S. (MB) \downarrow
UNCOMPRESSED (OURS)	-	18.1	942
QAT 8BITS	-	18.2	236
QAT 4BITS	-	28.8	118
DIFFQ ($\lambda=1, g=16$)	-	18.0	182
DIFFQ ($\lambda=10, g=16$)	-	18.5	113
8 BITS	8 BITS	19.5	236
QAT 8BITS	8 BITS	26.0	236
QAT 4BITS	8 BITS	34.6	118
DIFFQ ($\lambda=1, g=16$)	8 BITS	19.1	182
DIFFQ ($\lambda=10, g=16$)	8 BITS	19.2	113
UNCOMPRESSED \dagger	-	18.3	942
QN 8 BITS \dagger	QN 8 BITS	18.7	236
QN 4 BITS \dagger	QN 8 BITS	20.5	118